IEEE Photonics Journal
An IEEE Photonics Society Publication

Open Access

Power Adaptation Based on Truncated Channel Inversion for Hybrid FSO/RF Transmission With Adaptive Combining

Volume 7, Number 4, August 2015

Tamer Rakia, Student Member, IEEE
Hong-Chuan Yang, Senior Member, IEEE
Fayez Gebali, Senior Member, IEEE
Mohamed-Slim Alouini, Fellow, IEEE

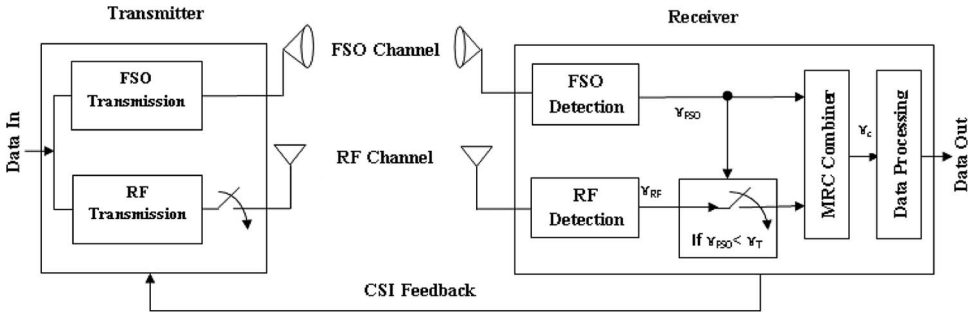

DOI: 10.1109/JPHOT.2015.2460118
1943-0655

Power Adaptation Based on Truncated Channel Inversion for Hybrid FSO/RF Transmission With Adaptive Combining

Tamer Rakia,[1] ***Student Member, IEEE*,**
Hong-Chuan Yang,[1] ***Senior Member, IEEE*,**
Fayez Gebali,[1] ***Senior Member, IEEE*, and**
Mohamed-Slim Alouini,[2] ***Fellow, IEEE***

[1]Department of Electrical and Computer Engineering, University of Victoria, Victoria, BC V8P 5C2, Canada
[2]Department of Electrical Engineering, King Abdullah University of Science and Technology, Thuwal 23955-6900, Saudi Arabia

DOI: 10.1109/JPHOT.2015.2460118

Manuscript received June 4, 2015; revised July 14, 2015; accepted July 18, 2015. Date of publication July 23, 2015; date of current version August 5, 2015. Corresponding author: T. Rakia (e-mail: tamer_nabiel@yahoo.com).

Abstract: Hybrid free-space optical (FSO)/radio-frequency (RF) systems have emerged as a promising solution for high-data-rate wireless communications. In this paper, we consider power adaptation strategies based on truncated channel inversion for the hybrid FSO/RF system employing adaptive combining. Specifically, we adaptively set the RF link transmission power when FSO link quality is unacceptable to ensure constant combined signal-to-noise ratio (SNR) at the receiver. Two adaptation strategies are proposed. One strategy depends on the received RF SNR, whereas the other one depends on the combined SNR of both links. Analytical expressions for the outage probability of the hybrid system with and without power adaptation are obtained. Numerical examples show that the hybrid FSO/RF system with power adaptation achieves a considerable outage performance improvement over the conventional system.

Index Terms: Hybrid free-space optical (FSO)/radio-frequency (RF), Gamma–Gamma atmospheric turbulence model, pointing errors, Nakagami-*m* fading model, outage probability, maximal ratio combining (MRC), power adaptation.

1. Introduction

Free-space optical (FSO) communication systems can achieve higher data rate compared to radio frequency (RF) systems, while their deployments are faster and cheaper than fiber optics. However, FSO systems suffer from atmospheric turbulence, pointing errors, and atmospheric loss due to unfavorable weather conditions. Turbulence-induced fading, known as scintillation, causes irradiance fluctuations in the received optical signal as a result of variations in the atmospheric refractive index. Misalignment between the transmitter and the receiver, known as pointing error effect, reduces the received optical power. Moreover, the optical power is also attenuated dramatically in fogy environment due to the atmospheric loss. One solution to improve the FSO link's reliability is to integrate it with a millimeter wavelength (MMW) radio frequency (RF) link and form a hybrid FSO/RF communication system. When a switch-over scheme is applied to hybrid FSO/RF systems (see [2] and references therein), hardware switching between FSO and MMW RF links is implemented to make use of their

complementary natures. This approach will lead to frequent hardware switching between the FSO and RF links [1]. Another implementation strategy is soft-switching (see [3] and references therein), which requires FSO and RF links to be active continuously, even when the FSO link has very good quality and can support the required bit-error rate (BER) by itself. In this scenario, RF transmission power is wasted, and the system generates unnecessary RF interference to the environment.

When the transmitter and the receiver are provided with channel state information (CSI), the transmission schemes can be adaptively selected to use the channel more efficiently. Power adaptation offers a simple but effective solution to improve link reliability and data throughput. Previous work on hybrid FSO/RF systems with power adaptation includes [4] and [5]. In particular, in [4] a hybrid FSO/RF system is considered, in which the system switches to the reliable RF link if the FSO link is obscured to maintain communication, and a water-filling power adaptation scheme is applied only on the FSO link. In [5], power adaptation has been applied on both FSO and RF links of the hybrid FSO/RF system, assuming that both links are active all the time but are transmitting with different rates.

To complement previous work on practical implementations of hybrid FSO/RF systems, we introduce, in this paper, a new power adaptation scheme for hybrid FSO/RF systems with adaptive combining. In this scheme, FSO link with high data rate is used alone for data transmission as long as its quality is acceptable and the RF link is put on standby mode. When FSO link's quality becomes poor and cannot support the high data rate, a feedback signal is sent along the FSO link to activate the RF link for simultaneous FSO/RF link data transmission. At the receiver terminal, maximal ratio combining (MRC) of signals received from both links is applied. In this case, system may lower the transmission rate of FSO link to be the same as that of RF link, to facilitate diversity reception. When the RF link is activated, the transmit power over the RF link is adapted according to a modified truncated channel inversion (TCI) power adaptation policy, such that the MRC combination of the RF and FSO links maintains a constant received signal-to-noise ratio (SNR). Since both FSO and MMW RF channels experience slow-fading [5], [6], we can assume that instantaneous CSI is always available at the receiver of both links, and there is a feedback channel for CSI feedback. When the quality of the FSO link alone becomes acceptable again, the RF link is put on standby mode again to save its power and spectrum utilization. In this paper, we propose two different power adaptation schemes for RF link. In both schemes, the RF power is adapted such that the MRC combination of the RF and FSO links can support the target received SNR. However, in the first scheme, the RF power is adapted as long as the received RF SNR is above a certain cutoff fade depth. Otherwise, data transmission is suspended. In the second one, the RF power is adapted as long as the combined SNR of the RF and FSO links is above another certain cutoff fade depth.

This hybrid FSO/RF system with RF link power adaptation is more reliable and power efficient as the RF link is activated only when the FSO link alone can not support high data rate. Thus, with the proposed power adaptation scheme, we have the advantage of maintaining constant received SNR while conserving RF power. Numerical results show that the hybrid system with power adaptation has superior outage performance compared to outage performance of the same system without power adaptation. Also, numerical results show that, somewhat counter intuition, the power adaptation scheme based on RF link SNR only has better outage performance than the scheme based on combined SNR.

The remainder of the paper is organized as follows. In Section 2, we introduce the system and channel models. In Section 3, we introduce the power allocation strategies and the outage analysis of the proposed system, namely, the outage probability and the outage capacity. Finally, Section 4 presents some numerical examples to investigate the performance of the hybrid system with and without power adaptation. Further power adaptation for FSO link is introduced in Section 5, followed by the conclusion in Section 6.

2. System and Channel Models

We consider a hybrid FSO/RF system where the FSO link is active all the time with constant transmitted power. To maintain a target data rate, the received SNR should not be less than a

predetermined target value denoted by γ_T. When the instantaneous SNR at the receiver of the FSO link, denoted by γ_{FSO}, falls below the threshold γ_T, FSO link alone cannot support the high data rate transmission. In this case, the receiver sends a feedback signal on the FSO link to activate the RF link along with the FSO link to help maintain the link reliability. When the RF link is activated, simultaneous transmission of the same data on both links takes place. At the receiver, the data received over both links will be combined using an MRC combiner. It is important to clarify that in case of using both FSO and RF links, the data rate of FSO link may be reduced to be the same as that of the RF link to facilitate diversity reception. The receiver SNR, denoted by γ_c, will be equal to γ_{FSO} when $\gamma_{\text{FSO}} \geq \gamma_T$. When $\gamma_{\text{FSO}} < \gamma_T$, γ_c will be equal to the sum of γ_{FSO} and γ_{RF} where γ_{RF} is the receiver SNR of the RF link. In this case, the transmitted power over the RF link is adapted to maintain the constant received SNR γ_T, i.e., to keep $\gamma_{\text{FSO}} + \gamma_{\text{RF}} = \gamma_T$. We will discuss the power adaptation policy in the following section.

2.1. Modeling the FSO Link

We assume that the FSO link experiences Gamma–Gamma fading due to atmospheric turbulence, and atmospheric loss along with pointing error impairments, for which the probability density function (PDF) of the received irradiance I is given by [10, Eq. (11)] (or equivalently using [11, Eq. (9.31.5)])

$$f_I(I) = \frac{\xi^2 I^{-1}}{\Gamma(\alpha)\Gamma(\beta)} G_{1,3}^{3,0}\left[\frac{\alpha\beta I}{A_0 h_L}\Big|_{\xi^2,\alpha,\beta}^{\xi^2+1}\right], \quad I \geq 0 \tag{1}$$

where ξ is the ratio between the equivalent beam radius at the FSO receiver aperture and the pointing error (jitter) standard deviation at the FSO receiver, A_0 is a constant term that defines the pointing error loss [6], $\Gamma(.)$ is the standard Gamma function, and α and β are the effective number of small-scale and large-scale eddies of the turbulent environment, respectively. Different values of α and β corresponds to different turbulence regimes. Expressions for calculating the parameters α and β for different propagation conditions can be found in [12]. In (1), $G[.]$ is the Meijer G-function as defined in [11, Eq. (9.301)], and h_L is the atmospheric loss over a propagation path of length z, determined by the exponential Beers-Lambert law as $h_L(z) = \exp(-\sigma z)$, with σ being the attenuation coefficient. The atmospheric loss depends on the visibility of the atmosphere and is considered constant [6].

Considering sub-carrier modulated FSO communication system, in which an electrical sub-carrier signal is pre-modulated[1] with the information bits before being used to modulate the optical signal for transmission, there are two techniques for FSO signal detection at the receiver side, which are heterodyne detection (coherent detection) and intensity modulation/direct detection (IM/DD). A unified expression for the PDF of γ_{FSO}, considering the two types of FSO detection, is given in a general form as [13]

$$f_{\gamma_{\text{FSO}}}(\gamma_{\text{FSO}}) = \frac{\xi^2 {\gamma_{\text{FSO}}}^{-1}}{r\Gamma(\alpha)\Gamma(\beta)} G_{1,3}^{3,0}\left[\frac{\xi^2\alpha\beta}{(\xi^2+1)}\left(\frac{\gamma_{\text{FSO}}}{\bar{\gamma}_{\text{FSO}_r}}\right)^{\frac{1}{r}}\Big|_{\xi^2,\alpha,\beta}^{\xi^2+1}\right], \quad \gamma_{\text{FSO}} \geq 0 \tag{2}$$

where r is the parameter defining the type of FSO detection technique (i.e., $r = 1$ represents heterodyne detection, and $r = 2$ represents IM/DD detection), and $\bar{\gamma}_{\text{FSO}_r}$[2] is the average SNR of FSO link.

[1] for example, by using the M-QAM digital modulation scheme, which is widely used in high-rate data transmissions over FSO links [7] and RF links [8] because of its high spectral efficiency and ease of signal modulation/demodulation process.

[2] For heterodyne FSO detection, $\bar{\gamma}_{FSO_1} = \eta_e E[I]/N_0$ [13], with η_e is the effective photoelectric conversion ratio, N_0 symbolizes the additive white Gaussian noise (AWGN) sample, and $E[I]$ is the expectation of I, which by using [14, Eq. (24)] is given by $E[I] = \xi^2 A_0 h_L/(\xi^2+1)$. For IM/DD FSO detection, $\bar{\gamma}_{\text{FSO}_2} = (\eta_e E[I])^2/N_0$ [13].

By using [15, Eq. (07.34.21.0084.01)] and some simple algebraic manipulations, the cumulative distribution function (CDF) of γ_{FSO} can be expressed as

$$F_{\gamma_{\text{FSO}}}(\gamma_{\text{FSO}}) = \frac{\xi^2 r^{\alpha+\beta-2}}{(2\pi)^{r-1}\Gamma(\alpha)\Gamma(\beta)} G_{r+1,3r+1}^{3r,1}\left[\frac{B\gamma_{\text{FSO}}}{\bar{\gamma}_{\text{FSO}_r}}\Big|_{K_2,0}^{1,K_1}\right], \quad \gamma_{\text{FSO}} \geq 0 \tag{3}$$

where $B = (\xi^2\alpha\beta/(\xi^2+1)r^2)^r$, $K_1 = (\xi^2+1)/r, \ldots, (\xi^2+r)/r$ has r terms, and $K_2 = \xi^2/r, \ldots, (\xi^2+r-1)/r, \alpha/r, \ldots, (\alpha+r-1)/r, \beta/r, \ldots, (\beta+r-1)/r$ has $3r$ terms.

2.2. Modeling the RF Link

At the RF transmitter, the digitally modulated electrical signal, which is the same as the one in FSO subsystem, is up-converted using 60 GHz RF carrier. The up-converted RF signal is transmitted and received using L branches RF transmission/reception scheme. The received SNR from each RF branch, denoted by $\gamma_{i_{\text{RF}}}$, follows independent and identical distribution (i.i.d) Nakagami-m fading distribution with PDF given by [16]

$$f_{\gamma_{i_{\text{RF}}}}(\gamma_{\text{RF}}) = \left(\frac{m}{\bar{\gamma}_{\text{RF}}}\right)^m \frac{\gamma_{\text{RF}}{}^{m-1}}{\Gamma(m)} \exp\left(\frac{-m\gamma_{\text{RF}}}{\bar{\gamma}_{\text{RF}}}\right), \quad \gamma_{\text{RF}} \geq 0 \tag{4}$$

where $\bar{\gamma}_{\text{RF}}$ is the average SNR of the ith channel with $1 \leq i \leq L$, and m is a parameter indicating fading severity. $\bar{\gamma}_{\text{RF}}$ and m are assumed to be common on all the L diversity branches. The overall received SNR of the RF link γ_{RF} will be that after the MRC combination of all the L RF channels, such that $\gamma_{\text{RF}} = \sum_{i=1}^{L} \gamma_{i_{\text{RF}}}$, the PDF of which is given by [16]

$$f_{\gamma_{\text{RF}}}(\gamma_{\text{RF}}) = \left(\frac{m}{\bar{\gamma}_{\text{RF}}}\right)^{mL} \frac{\gamma_{\text{RF}}{}^{mL-1}}{\Gamma(mLm)} \exp\left(\frac{-m\gamma_{\text{RF}}}{\bar{\gamma}_{\text{RF}}}\right), \quad \gamma_{\text{RF}} \geq 0. \tag{5}$$

By using [11, Eq. (3.351.1)], and some simple algebraic manipulations, the CDF of γ_{RF} can be expressed as

$$F_{\gamma_{\text{RF}}}(\gamma_{\text{RF}}) = \frac{1}{\Gamma(mL)} \gamma\left(mL, \frac{m\gamma_{\text{RF}}}{\bar{\gamma}_{\text{RF}}}\right), \quad \gamma_{\text{RF}} \geq 0 \tag{6}$$

where $\gamma(a, x)$ is the lower incomplete Gamma function defined in [11, Eq. (8.350.1)].

3. Power Allocation Strategies and Outage Analysis

We assume constant FSO transmitting power all the time. When $\gamma_{\text{FSO}} < \gamma_T$, the RF link is activated along with the FSO link and the RF link transmitted power P_{RF} is adapted to maintain the required constant received SNR γ_T. We introduce here two different policies for RF link power adaptation. Both of them are based on the TCI principle [17].

3.1. TCI For RF Link Based on γ_{RF}

3.1.1. Power Adaptation Policy

In this power adaptation policy, the transmitter uses the CSI (specifically, γ_{FSO} and γ_{RF}) to maintain the target received SNR γ_T. Since the power adaptation is performed after activating the RF link, the RF link SNR is adaptively changed to fill the gap between γ_{FSO} and γ_T such that $\gamma_{\text{RF}} + \gamma_{\text{FSO}} = \gamma_T$. The RF power is adapted as long as the received RF SNR is above a certain threshold denoted by γ_{0_l}. Otherwise, data transmission is suspended. We will refer to this policy as γ_{RF}-based TCI, which is mathematically given by

$$\frac{P_{\text{RF}}(\gamma_{\text{RF}}, \gamma_{\text{FSO}})}{\bar{P}_{\text{RF}}} = \begin{cases} \frac{\gamma_T - \gamma_{\text{FSO}}}{\gamma_{\text{RF}}}, & \text{if } \gamma_{\text{RF}} \geq \gamma_{0_l} \\ 0, & \text{if } \gamma_{\text{RF}} < \gamma_{0_l} \end{cases} \tag{7}$$

where γ_{0_I} satisfies the average power constraint of RF link transmitter given by

$$\int_0^{\gamma_T}\int_{\gamma_{0_I}}^{\infty}\frac{P_{\mathrm{RF}}(\gamma_{\mathrm{RF}},\gamma_{\mathrm{FSO}})}{\bar{P}_{\mathrm{RF}}}f_{\gamma_{\mathrm{RF}}}(\gamma_{\mathrm{RF}})f_{\gamma_{\mathrm{FSO}}}(\gamma_{\mathrm{FSO}})d\gamma_{\mathrm{RF}}d\gamma_{\mathrm{FSO}}=1 \tag{8}$$

where $\bar{P}_{\mathrm{RF}}$ is the average transmitted power over the RF link.

By substituting (2) and (5) in (8), and using [11, Eq. (3.381.9)] and [15, Eq. (07.34.21.0084.01)], the constraint in (8) can be expressed as

$$A_1\Gamma\left(mL-1,\frac{m\gamma_{0_I}}{\bar{\gamma}_{\mathrm{RF}}}\right)\left\{G_{r+1,3r+1}^{3r,1}\left[\frac{B\gamma_T}{\bar{\gamma}_{\mathrm{FSO}_r}}\Big|_{K_2,0}^{1,K_1}\right]-G_{r+1,3r+1}^{3r,1}\left[\frac{B\gamma_T}{\bar{\gamma}_{\mathrm{FSO}_r}}\Big|_{K_2,-1}^{0,K_1}\right]\right\}=1 \tag{9}$$

where $A_1=\xi^2 r^{\alpha+\beta-2}m\gamma_T/(2\pi)^{r-1}\bar{\gamma}_{RF}\Gamma(\alpha)\Gamma(\beta)\Gamma(mL)$, and $\Gamma(a,x)$ is the upper incomplete Gamma function defined in [11, Eq. (8.350.2)]. As with most TCI schemes, the value for γ_{0_I} that satisfies (9) can be found using numerical methods, such as bisection method and Newton method [18].

3.1.2. Outage Probability For γ_{RF}-Based TCI

According to this policy, the hybrid system goes into outage state if the RF link received SNR γ_{RF} goes below γ_{0_I}. The probability of outage in this case can be calculated as

$$\begin{aligned}\mathrm{P}_{\mathrm{out}}&=\mathrm{P}_{\mathrm{r}}[\gamma_{\mathrm{FSO}}<\gamma_T]\mathrm{P}_{\mathrm{r}}[\gamma_{\mathrm{RF}}<\gamma_{0_I}].\\&=F_{\gamma_{\mathrm{FSO}}}(\gamma_T)F_{\gamma_{\mathrm{RF}}}(\gamma_{0_I})\end{aligned} \tag{10}$$

where $F_{\gamma_{\mathrm{FSO}}}(.)$ and $F_{\gamma_{\mathrm{RF}}}(.)$ are given by (3) and (6), respectively.

3.2. TCI For RF Link Based on $\gamma_{RF}+\gamma_{FSO}$

3.2.1. Power Adaptation Policy

This RF link power adaptation policy is similar to the first one. However, the RF power is adapted as long as the overall SNR after MRC combination of the RF link and the FSO link (i.e., $\gamma_{\mathrm{RF}}+\gamma_{\mathrm{FSO}}$) is above a certain threshold denoted by $\gamma_{0_{II}}$. Otherwise, data transmission is suspended. We will refer to this policy as $\gamma_{\mathrm{RF}}+\gamma_{\mathrm{FSO}}$-based TCI which is given by

$$\frac{P_{\mathrm{RF}}(\gamma_{\mathrm{RF}},\gamma_{\mathrm{FSO}})}{\bar{P}_{\mathrm{RF}}}=\begin{cases}\frac{\gamma_T-\gamma_{\mathrm{FSO}}}{\gamma_{\mathrm{RF}}}, & \text{if } \gamma_{\mathrm{RF}}+\gamma_{\mathrm{FSO}}\geq\gamma_{0_{II}}\\ 0, & \text{if } \gamma_{\mathrm{RF}}+\gamma_{\mathrm{FSO}}<\gamma_{0_{II}}\end{cases} \tag{11}$$

where $\gamma_{0_{II}}$ satisfies the average power constraint over the RF link given by

$$\int_0^{\gamma_T}\int_{\gamma_{0_{II}}-\gamma_{\mathrm{FSO}}}^{\infty}\frac{P_{\mathrm{RF}}(\gamma_{\mathrm{RF}},\gamma_{\mathrm{FSO}})}{\bar{P}_{\mathrm{RF}}}f_{\gamma_{\mathrm{RF}}}(\gamma_{\mathrm{RF}})f_{\gamma_{\mathrm{FSO}}}(\gamma_{\mathrm{FSO}})d\gamma_{\mathrm{RF}}d\gamma_{\mathrm{FSO}}=1. \tag{12}$$

By substituting (2) and (5) in (12), and using the binomial expansion defined in [11, Eq. (1.111)] and the series expansion of the exponential defined in [11, Eq. (1.211.1)], along with [11, Eq. (3.351.2)] and [15, Eq. (07.34.21.0084.01)], the constraint in (12) can be expressed as

$$\begin{aligned}A_2e^{\frac{-m\gamma_{0_{II}}}{\bar{\gamma}_{\mathrm{RF}}}}\sum_{n=0}^{\infty}\frac{(m\gamma_T/\bar{\gamma}_{\mathrm{RF}})^n}{n!}\sum_{i=0}^{mL-2}\frac{(m\gamma_{0_{II}}/\bar{\gamma}_{\mathrm{RF}})^i}{i!}\sum_{k=0}^{i}\binom{i}{k}\left(\frac{-\gamma_T}{\gamma_{0_{II}}}\right)^k\left\{G_{r+1,3r+1}^{3r,1}\left[\frac{B\gamma_T}{\bar{\gamma}_{\mathrm{FSO}_r}}\Big|_{K_2,-n-k}^{1-n-k,K_1}\right]\right.\\\left.-G_{r+1,3r+1}^{3r,1}\left[\frac{B\gamma_T}{\bar{\gamma}_{\mathrm{FSO}_r}}\Big|_{K_2,-n-k-1}^{-n-k,K_1}\right]\right\}=1\end{aligned} \tag{13}$$

where $A_2=\xi^2 r^{\alpha+\beta-2}m(mL-2)!\gamma_T/(2\pi)^{r-1}\bar{\gamma}_{\mathrm{RF}}\Gamma(\alpha)\Gamma(\beta)\Gamma(mL)\bar{\gamma}_{\mathrm{RF}}$. Similar to γ_{0_I}, the value for $\gamma_{0_{II}}$ that satisfies (13) can be found using numerical methods. When using (13) to search for the value

TABLE 1
Values of $\gamma_{0_{II}}$ Considering Heterodyne FSO Detection $(r = 1)$ With Different Values of n

$\bar{\gamma}_{RF}$ (dB)	$n = 30$	$n = 35$	$n = 40$	$n = 45$
0	6.2125	6.2142	6.2142	6.2142
1	5.5250	5.5250	5.5251	5.5251
8	4.3291	4.3291	4.3291	4.3291
12	1.9091	1.9091	1.9091	1.9091

TABLE 2
Values of $\gamma_{0_{II}}$ Considering IM/DD FSO Detection $(r = 2)$ With Different Values of n

$\bar{\gamma}_{RF}$ (dB)	$n = 30$	$n = 35$	$n = 40$	$n = 45$
0	7.2243	7.2264	7.2265	7.2265
4	4.9315	4.9315	4.9315	4.9315
10	3.5144	3.5144	3.5144	3.5144
12	1.2882	1.2882	1.2882	1.2882

of $\gamma_{0_{II}}$, it is sufficient to use $n = 40$ to obtain stable values with accuracy to the fourth digit. This can be observed from Tables 1 and 2, where we consider $\gamma_T = 10$ dB, typical values of α and β for weak atmospheric turbulence regime ($\alpha = 2.902$, and $\beta = 2.51$) [21], $\bar{\gamma}_{\mathrm{FSO}_r} = 0$ dB, $\xi = 1$, Nakagami parameter $m = 2$, and $L = 1$ to obtain the values of $\gamma_{0_{II}}$ for different values of $\bar{\gamma}_{\mathrm{RF}}$.

3.2.2. Outage Probability for $\gamma_{RF} + \gamma_{FSO}$-Based TCI

According to this policy, the hybrid system goes into outage state if MRC combination of the FSO and RF links failed to support a received SNR of $\gamma_{\mathrm{RF}} + \gamma_{\mathrm{FSO}} \geq \gamma_{0_{II}}$. The probability of outage in this case can be calculated as

$$\begin{aligned} \mathrm{P}_{\mathrm{out}} &= \mathrm{P}_{\mathrm{r}}[\gamma_{\mathrm{FSO}} < \gamma_T, \gamma_{\mathrm{FSO}} + \gamma_{\mathrm{RF}} < \gamma_{0_{II}}]. \\ &= \int_0^{\gamma_{0_{II}}} \int_0^{\min[\gamma_T, \gamma_{0_{II}} - \gamma_{\mathrm{RF}}]} f_{\gamma_{\mathrm{FSO}}}(\gamma_{\mathrm{FSO}}) f_{\gamma_{\mathrm{RF}}}(\gamma_{\mathrm{RF}}) d\gamma_{\mathrm{FSO}} d\gamma_{\mathrm{RF}}. \\ &= \int_0^{\gamma_{0_{II}} - \gamma_T} \int_0^{\gamma_T} f_{\gamma_{\mathrm{FSO}}}(\gamma_{\mathrm{FSO}}) f_{\gamma_{\mathrm{RF}}}(\gamma_{\mathrm{RF}}) d\gamma_{\mathrm{FSO}} d\gamma_{\mathrm{RF}} \\ &\quad + \int_{\gamma_{0_{II}} - \gamma_T}^{\gamma_{0_{II}}} \int_0^{\gamma_{0_{II}} - \gamma_{\mathrm{RF}}} f_{\gamma_{\mathrm{FSO}}}(\gamma_{\mathrm{FSO}}) f_{\gamma_{\mathrm{RF}}}(\gamma_{\mathrm{RF}}) d\gamma_{\mathrm{FSO}} d\gamma_{\mathrm{RF}}. \end{aligned} \tag{14}$$

If $\gamma_T > \gamma_{0_{II}}$, which is the case most of the time, then (14) will be given by

$$\begin{aligned} \mathrm{P}_{\mathrm{out}} &= \int_0^{\gamma_{0_{II}}} \int_0^{\gamma_{0II}-\gamma_{\mathrm{RF}}} f_{\gamma_{\mathrm{FSO}}}(\gamma_{\mathrm{FSO}}) f_{\gamma_{\mathrm{RF}}}(\gamma_{\mathrm{RF}}) d\gamma_{\mathrm{FSO}} d\gamma_{\mathrm{RF}}. \\ &= \int_0^{\gamma_{0_{II}}} f_{\gamma_{\mathrm{RF}}}(\gamma_{\mathrm{RF}}) F_{\gamma_{\mathrm{FSO}}}(\gamma_{0_{II}} - \gamma_{\mathrm{RF}}) d\gamma_{\mathrm{RF}}. \end{aligned} \tag{15}$$

By substituting (3) and (5) in (15), making change of variable, and using the series expansion of the exponential, along with [15, Eq. (07.34.21.0084.01)], (15) can be evaluated as

$$\mathrm{P}_{\mathrm{out}} = \frac{\xi^2 r^{\alpha+\beta-2} e^{\frac{-m\gamma_{0_{II}}}{\bar{\gamma}_{\mathrm{RF}}}} \left(\frac{m\gamma_{0_{II}}}{\bar{\gamma}_{\mathrm{RF}}}\right)^{mL}}{(2\pi)^{r-1}\Gamma(\alpha)\Gamma(\beta)} \sum_{n=0}^{\infty} \left\{ \frac{\left(\frac{m\gamma_{0_{II}}}{\bar{\gamma}_{\mathrm{RF}}}\right)^{n}}{n!} G_{r+2,3r+2}^{3r,2}\left[\frac{B\gamma_{0_{II}}}{\bar{\gamma}_{\mathrm{FSO}_r}} \Big|_{K_2,0,-n-mL}^{-n,1,K_1}\right] \right\}. \tag{16}$$

3.3. Outage Capacity

Practically speaking, outage capacity applies to slowly-varying channels [17], which is the case with FSO and MMW RF channels with bit-duration much smaller than the channels coherence time [5], [6]. The outage capacity is defined as the maximum data rate that can be maintained in all non-outage channel states times the probability of non-outage. The outage capacity associated with a given outage probability $\mathrm{P}_{\mathrm{out}}$ normalized to the communication channel bandwidth B can be expressed as [19]

$$\frac{C(\mathrm{P}_{\mathrm{out}})}{B} = [1 - \mathrm{P}_{\mathrm{out}}]\log_2(1 + K\gamma_T) \tag{17}$$

where K is a constant term such that $K = 1$ for heterodyne detection giving an exact result, and $K = e/(2\pi)$ for IM/DD giving a lower-bound result. The outage probability P_{out} in (17) is given by either (10) or (16) according to the power adaptation policy used on the RF link.

4. Numerical Results

In this section, we present several numerical examples to investigate the performance of the two proposed power adaptation strategies. Note that in all numerical results, we assume using optical wavelength $\lambda_{\mathrm{FSO}} = 1550$ nm [20]. In addition, note that for the numerical results shown in Figs. 1, 4, and 5, we assume no RF diversity, i.e., $L = 1$.

In Fig. 1, we plot the outage probability of the hybrid system with and without power adaptation as a function of the average RF link SNR $\bar{\gamma}_{\mathrm{RF}}$. We assume weak atmospheric turbulence ($\alpha = 2.902$, and $\beta = 2.51$) affecting the FSO link with pointing error effect of $\xi = 1$, and RF link fading severity of $m = 2$. It can be seen from Fig. 1 that considering either heterodyne FSO detection technique [Fig. 1(a)] or IM/DD FSO detection technique [Fig. 1(b)], using the γ_{RF}-based TCI adaptation policy gives better outage performance than using the $\gamma_{\mathrm{RF}} + \gamma_{\mathrm{FSO}}$-based TCI adaptation policy. This is because that under the same conditions of the FSO and RF links, γ_{0_I} is less than $\gamma_{0_{II}}$. To explain this, let $f(\gamma_{\mathrm{RF}}, \gamma_{\mathrm{FSO}}) = (P_{\mathrm{RF}}(\gamma_{\mathrm{RF}}, \gamma_{\mathrm{FSO}})/\bar{P}_{\mathrm{RF}}) f_{\gamma_{\mathrm{RF}}}(\gamma_{\mathrm{RF}}) f_{\gamma_{\mathrm{FSO}}}(\gamma_{\mathrm{FSO}})$. We need the integration of $f(\gamma_{\mathrm{RF}}, \gamma_{\mathrm{FSO}})$ over the red shaded area in Fig. 2 to be equal to 1, according to (8), and also we need the integration of $f(\gamma_{\mathrm{RF}}, \gamma_{\mathrm{FSO}})$ over the black shaded area in Fig. 2 to be equal to 1, according to (12). If we assume that γ_{0_I} is greater than or equal to $\gamma_{0_{II}}$, then the integration of $f(\gamma_{\mathrm{RF}}, \gamma_{\mathrm{FSO}})$ over the red shaded area will be greater than 1 which is impossible according to the constraint in (8). Thus, γ_{0_I} is less than $\gamma_{0_{II}}$. The analytical results for the outage probability of the hybrid system with $\gamma_{\mathrm{RF}} + \gamma_{\mathrm{FSO}}$-based TCI adaptation policy shown in Fig. 1 are obtained using $n = 30$ in (16). As can be observed, evaluating the outage probability with the truncated values of $n = 30$ gives accurate results, as compared with the values obtained by

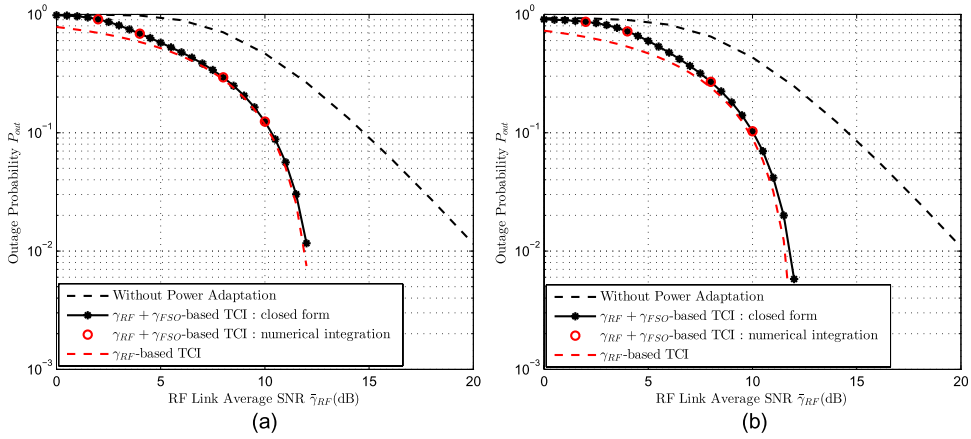

Fig. 1. Outage probability of hybrid FSO/RF system with and without power adaptation as a function of the average SNR of the RF link with $\gamma_T = 10$ dB, weak atmospheric turbulence ($\alpha = 2.902$, and $\beta = 2.51$), $\bar{\gamma}_{\text{FSO}_r} = 0$ dB, $\xi = 1$, and Nakagami parameter $m = 2$. (a) Using heterodyne detection technique with FSO link $(r = 1)$. (b) Using IM/DD detection technique with FSO link $(r = 2)$.

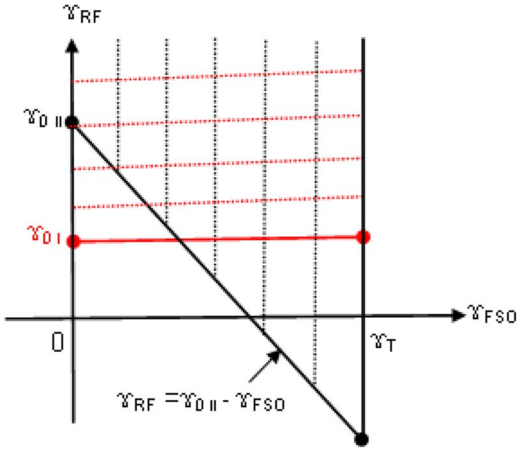

Fig. 2. Integration regions of (8) and (12).

evaluating the integral in (15) using numerical methods. It can also be seen from Fig. 1 that applying power adaptation (either γ_{RF}-based TCI or $\gamma_{\text{RF}} + \gamma_{\text{FSO}}$-based TCI) policy greatly improves the outage performance of the hybrid system over the case without using power adaptation. Note that we had used numerical integration to evaluate the outage probability for the hybrid system without power adaptation, given in (21) in the Appendix, with outage threshold $\gamma_{\text{out}} = 9.5$ dB. Note also that the value $\gamma_{\text{out}} = 9.5$ dB is less than $\gamma_T = 10$ dB so that the hybrid system switches to the MRC combination of the FSO and RF links before the FSO link alone goes into outage.

In Fig. 3, we examine the effect of the RF link diversity on the outage performance of the hybrid FSO/RF system with both power adaptation policies [see Fig. 3(a) and (b)]. It can be seen from Fig. 3, that as the number of the RF branches increases, the outage performance of the hybrid system greatly improves. Intuitively, the same observation shown in Fig. 3 is also applicable when using heterodyne FSO detection technique.

In Fig. 4, we examine the outage performance of the proposed hybrid FSO/RF system in the presence of strong atmospheric turbulence ($\alpha = 2.064$, and $\beta = 1.342$) affecting the FSO link with less severe pointing error effect of $\xi = 4$, and RF link fading severity of $m = 2$. It can be

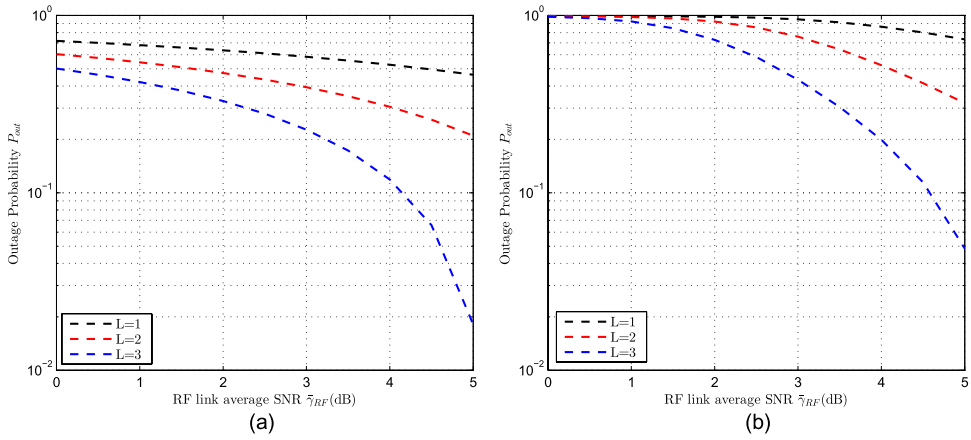

Fig. 3. Outage probability of hybrid FSO/RF system with power adaptation as a function of the average SNR of the RF link considering IM/DD FSO detection technique, with $\gamma_T = 10$ dB, weak atmospheric turbulence ($\alpha = 2.902$, and $\beta = 2.51$), $\bar{\gamma}_{\mathrm{FSO}_2} = 0$ dB, $\xi = 1$, and Nakagami parameter $m = 2$. (a) Using γ_{RF}-based TCI. (b) Using $\gamma_{\mathrm{RF}} + \gamma_{\mathrm{FSO}}$-based TCI.

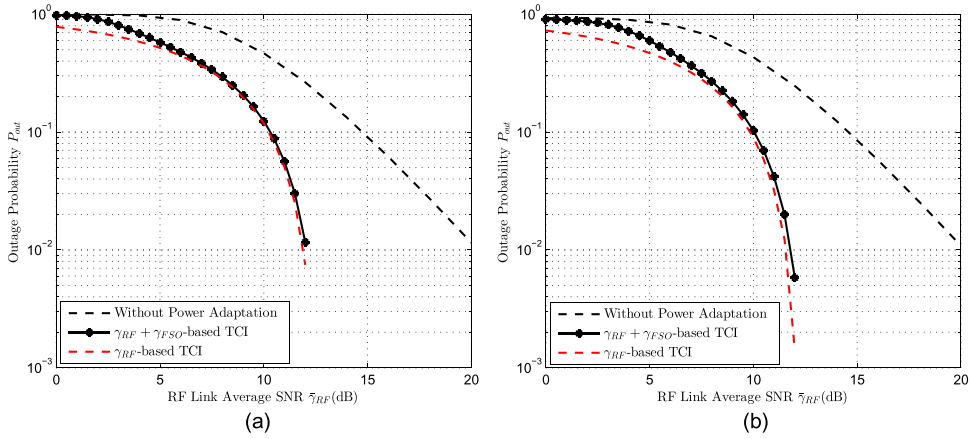

Fig. 4. Outage probability of hybrid FSO/RF system with and without power adaptation as a function of the average SNR of the RF link with $\gamma_T = 10$ dB, strong atmospheric turbulence ($\alpha = 2.064$, and $\beta = 1.342$), $\bar{\gamma}_{\mathrm{FSO}_r} = 0$ dB, $\xi = 4$, and Nakagami parameter $m = 2$. (a) Using heterodyne detection technique with FSO link $(r = 1)$. (b) Using IM/DD detection technique with FSO link $(r = 2)$.

seen from Fig. 4 that the hybrid FSO/RF system employing either of the two proposed power adaptation polices achieves superior outage performance compared to the performance of the system without power adaptation in this case as well.

In Fig. 5, we plot the outage capacity of the hybrid system with power adaptation as a function of the average RF link SNR $\bar{\gamma}_{\mathrm{RF}}$. We assume weak atmospheric turbulence ($\alpha = 2.902$, and $\beta = 2.51$) affecting the FSO link with pointing error effect of $\xi = 1$, and RF link fading severity of $m = 2$. It can be seen from Fig. 5 that considering either heterodyne FSO detection technique [see Fig. 5(a)] or IM/DD FSO detection technique [see Fig. 5(b)], using γ_{RF}-based TCI adaptation policy leads to higher outage capacity than using $\gamma_{\mathrm{RF}} + \gamma_{\mathrm{FSO}}$-based TCI adaptation policy. This is because using γ_{RF}-based TCI adaptation policy achieves smaller outage probability than $\gamma_{\mathrm{RF}} + \gamma_{\mathrm{FSO}}$-based TCI adaptation policy. However, when $\bar{\gamma}_{\mathrm{RF}}$ becomes high, the outage capacity obtained when using $\gamma_{\mathrm{RF}} + \gamma_{\mathrm{FSO}}$-based TCI adaptation policy becomes the same as that obtained when using γ_{RF}-based TCI adaptation policy. This is because both $\gamma_{\mathrm{RF}} + \gamma_{\mathrm{FSO}}$-based TCI

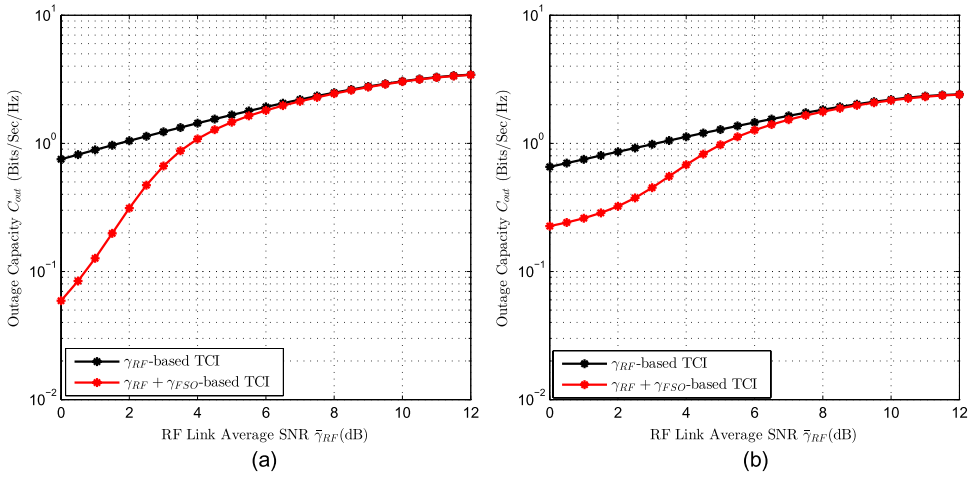

Fig. 5. Outage capacity of hybrid FSO/RF system with power adaptation as a function of the average SNR of the RF link with $\gamma_T = 10$ dB, weak atmospheric turbulence ($\alpha = 2.902$, and $\beta = 2.51$), $\bar{\gamma}_{\text{FSO}_r} = 0$ dB, $\xi = 1$, and Nakagami parameter $m = 2$. (a) Using heterodyne detection technique with FSO link ($r = 1$). (b) Using IM/DD detection technique with FSO link ($r = 2$).

adaptation policy and γ_{RF}-based TCI adaptation policy achieve almost the same outage probability with high values of $\bar{\gamma}_{\text{RF}}$.

5. Power Adaptation on FSO Link

To conserve more power, the transmit power over the FSO link can be adapted according to the following modified TCI policy

$$\frac{P_{\text{FSO}}(\gamma_{\text{FSO}})}{P_{\text{FSOmax}}} = \begin{cases} \frac{\gamma_T}{\gamma_{\text{FSO}}}, & \text{if } \gamma_{\text{FSO}} \geq \gamma_T \\ 1, & \text{if } \gamma_{\text{FSO}} < \gamma_T. \end{cases} \tag{18}$$

According to this power adaptation policy, FSO power denoted by P_{FSO} gradually increases when the FSO link is in good quality (i.e., $\gamma_{\text{FSO}} \geq \gamma_T$) to reach its maximum value of $P_{FSO\text{max}}$ when the FSO link quality is bad (i.e., $\gamma_{\text{FSO}} < \gamma_T$). In other words, we use constant FSO power of P_{FSOmax} when $\gamma_{\text{FSO}} < \gamma_T$. Thus, this additional power adaptation for FSO link can further improve the power efficiency of the hybrid FSO/RF system, while maintaining the same outage performance of the system.

6. Conclusion

In this paper, we introduced low complexity power adaptation strategy to hybrid FSO/RF systems with adaptive combining. Two power adaptation policies based on a modified TCI were implemented on the RF link of the hybrid system. We analyzed the outage performance of the proposed adaptive system, and closed forms for the outage probabilities were derived. Numerical results showed that the hybrid system with power adaptation has superior outage performance compared to outage performance of the same system without power adaptation, while conserving RF power. In addition, numerical results showed that γ_{RF}-based TCI adaptation policy achieves better outage performance than $\gamma_{\text{RF}} + \gamma_{\text{FSO}}$-based TCI adaptation policy.

Appendix

In this Appendix, we analyze the outage probability of the hybrid FSO/RF system without power adaptation. We assume that the outage threshold denoted by γ_{out} is smaller than the switching

threshold γ_T. Otherwise, the hybrid system will enter outage before activating RF link. When the FSO link SNR γ_{FSO} falls below γ_T, and the instantaneous receiver SNR $\gamma_c = \gamma_{\text{FSO}} + \gamma_{\text{RF}}$ falls below the outage threshold γ_{out}, the communication link cannot support a target BER and goes into the outage state. In this case, the outage probability of the hybrid FSO/RF system without power adaptation can be calculated as

$$\begin{aligned} \mathrm{P}_{\text{out}} &= \mathrm{P}_{\text{r}}[\gamma_{\text{FSO}} < \gamma_T, \gamma_{\text{FSO}} + \gamma_{\text{RF}} < \gamma_{\text{out}}] \\ &= \int_0^{\gamma_{\text{out}}} f_{\gamma_{\text{FSO}}+\gamma_{\text{RF}}}(y)\,dy. \end{aligned} \tag{19}$$

Noting that the FSO and RF links are statistically independent, $f_{\gamma_{\text{FSO}}+\gamma_{\text{RF}}}(y)$ in (19) can be evaluated as

$$f_{\gamma_{\text{FSO}}+\gamma_{\text{RF}}}(y) = \int_0^{y} f_{\gamma_{\text{FSO}}}(\gamma_{\text{FSO}}) f_{\gamma_{\text{RF}}}(y - \gamma_{\text{FSO}})\,d\gamma_{\text{FSO}} \tag{20}$$

where $f_{\gamma_{\text{FSO}}}(.)$ and $f_{\gamma_{\text{RF}}}(.)$ are given by (2) and (5), respectively. Finally

$$\mathrm{P}_{\text{out}} = \int_0^{\gamma_{\text{out}}} \int_0^{y} f_{\gamma_{\text{FSO}}}(\gamma_{\text{FSO}}) f_{\gamma_{\text{RF}}}(y - \gamma_{\text{FSO}})\,d\gamma_{\text{FSO}}\,dy \tag{21}$$

which can be numerically evaluated.

References

[1] S. Vangala and H. P. Nik, "Optimal hybrid RF–wireless optical communication for maximum efficiency and reliability," in *Proc. CISS*, Baltimore, MD, USA, Mar. 2007, pp. 684–689.

[2] M. Usman, H.-C. Yang, and M.-S. Alouini, "Practical switching-based hybrid FSO/RF transmission and its performance analysis," *IEEE Photon. J.* , vol. 6, no. 5, pp. 1–13, Oct. 2014.

[3] N. D. Chatzidiamantis, G. K. Karagiannidis, E. E. Kriezis, and M. Matthaiou, "Diversity combining in hybrid RF/FSO systems with PSK modulation," in *Proc. IEEE ICC*, Jun. 2011, pp. 1–6.

[4] H. Moradi, M. Falahpour, H. H. Refai, P. G. LoPresti, and M. Atiquzzaman, "On the capacity of hybrid FSO/RF links," in *Proc. IEEE Globecom*, Dec. 2010, pp. 1–5.

[5] N. Letzepis, K. Nguyen, A. G. Fabregas, and W. Cowley, "Outage analysis of the hybrid free-space optical and radio-frequency channel," *IEEE J. Sel. Areas Commun.*, vol. 27, no. 9, pp. 1709–1719, Dec. 2009. **AQ1**

[6] A. Farid and S. Hranilovic, "Outage capacity optimization for free-space optical links with pointing errors," *J. Lightw. Technol.*, vol. 25, no. 7, pp. 1702–1710, Jul. 2007.

[7] B. T. Vu, N. T. Dang, T. G. Thang, and A. T. Pham, "Bit error rate analysis of rectangular QAM/FSO systems using APD receiver over atmospheric turbulence channels," *J. Opt. Commun. Netw.*, vol. 5, no. 5, pp. 437–446, Apr. 2013.

[8] X. Lei, P. Fan, and L. Hao, "Exact symbol error probability of general order rectangular QAM with MRC diversity reception over Nakagami-*m* fading channels," *IEEE Commun. Lett.*, vol. 11, no. 12, pp. 958–960, Dec. 2007.

[9] I. E. Lee *et al.*, "Practical implementation and performance study of a hard-switched hybrid FSO/RF link under controlled fog environment," in *Proc. 9th Int. Symp. CSNDSP*, Manchester, U.K., 2014, pp. 368–373.

[10] H. Sandalidis, T. Tsiftsis, and G. Karagiannidis, "Optical wireless communication with heterodyne detection over turbulence channels with pointing errors," *J. Lightw. Technol.*, vol. 27, no. 20, pp. 4440–4445, Oct. 2009.

[11] I. S. Gradshteyn and I. M. Ryzhik, *Table of Integrals, Series, and Products*. Amsterdam, The Netherlands: Elsevier Academic, 2007.

[12] L. C. Andrews and R. L. Phillips, *Laser Beam Propagation Through Random Media*, 2nd ed. Bellingham, WA, USA, SPIE Opt. Eng., 2005.

[13] I. Ansari, F. Yilmaz, and M.-S. Alouini, "Performance analysis of FSO links over unified Gamma–Gamma turbulence channels," in *Proc. IEEE VTC—Spring*, Glasgow, U.K., May 2015, pp. 1–5.

[14] V. S. Adamchik and O. I. Marichev, "The algorithm for calculating integrals of hypergeometric type functions and its realization in REDUCE system," in *Proc. Int. Conf. Symb. Algebraic Comput.*, Tokyo, Japan, 1990, pp. 212–224.

[15] "Mathematica Edition," Wolfram Research, Inc., Champaign, IL, USA, Ver. 8.0., 2010.

[16] H.-C. Yang and M.-S. Alouini, *Order Statistics in Wireless Communication*. Cambridge, U.K.: Cambridge Univ. Press, 2011.

[17] A. Goldsmith, *Wireless Communication*, 5th ed. Cambridge, MA, USA: Cambridge Univ. Press, 2005.

[18] A. Antoniou and W.-S. Lu, *Practical Optimization: Algorithms and Engineering Applications*. New York, NY, USA: Springer-Verlag, 2007.
[19] A. Lapidoth, S. M. Moser, and M. A. Wigger, "On the capacity of free-space optical intensity channels," *IEEE Trans. Inf. Theory*, vol. 55, no. 10, pp. 4449–4461, Oct. 2009.
[20] I. E. Lee, Z. Ghassemlooy, W. P. Ng, and M. Uysal, "Performance analysis of free space optical links over turbulence and misalignment induced fading channels," in *Proc. 8th Int. Symp. CSNDSP*, Poznan, Poland, 2012, pp. 1–6.
[21] X. Tang, Z. Ghassemlooy, S. Rajbhandari, W. O. Popoola, and C. G. Lee, "Coherent polarization shift keying modulated free space optical links over a Gamma–Gamma turbulence channel," *Amer. J. Appl. Sci.*, vol. 4, no. 4, pp. 520–530, Oct. 2011.